Pharmacokinetics of Ferumoxytol in the Abdomen and Pelvis: A Dosing Study with 1.5- and 3.0-T MRI Relaxometry

Wells, Shane A ; Schubert, Tilman ; Motosugi, Utaroh ; Sharma, Samir D ; Campo, Camilo A ; Kinner, Sonja ; Woo, Kaitlin M ; Hernando, Diego ; Reeder, Scott B

Abstract: Background The off-label use of ferumoxytol (FE), an intravenous iron preparation for iron deficiency anemia, as a contrast agent for MRI is increasing; therefore, it is critical to understand its pharmacokinetics. Purpose To evaluate the pharmacokinetics of FE in the abdomen and pelvis, as assessed with quantitative 1.5- and 3.0-T MRI relaxometry. Materials and Methods R2*, an MRI technique used to estimate tissue iron content in the abdomen and pelvis, was performed at 1.5 and 3.0 T in 12 healthy volunteers between April 2015 and January 2016. Volunteers were randomly assigned to receive an FE dose of 2 mg per kilogram of body weight (FE_{2mg}) or 4 mg/kg (FE_{4mg}). MRI was repeated at 1.5 and 3.0 T for each volunteer at five time points: days 1, 2, 4, 7, and 30. A radiologist experienced in MRI relaxometry measured R2* in organs of the mononuclear phagocyte system (MPS) (ie, liver, spleen, and bone marrow), non-MPS anatomy (kidney, pancreas, and muscle), inguinal lymph nodes (LNs), and blood pool. A paired Student t test was used to compare changes in tissue R2*. Results Volunteers (six female; mean age, 44.3 years ± 12.2 [standard deviation]) received either FE_{2mg} (n = 5) or FE_{4mg} (n = 6). Overall R2* trend analysis was temporally significant (P < .001). Time to peak R2* in the MPS occurred on day 1 for FE_{2mg} and between days 1 and 4 for FE_{4mg} (P < .001 to P < .002). Time to peak R2* in non-MPS anatomy, LNs, and blood pool occurred on day 1 for both doses (P < .001 to P < .09). Except for the spleen (at 1.5 T) and liver, MPS R2* remained elevated through day 30 for both doses (P = .02 to P = .03). Except for the kidney and pancreas, non-MPS, LN, and blood pool R2* returned to baseline levels between days 2 and 4 at FE_{2mg} (P = .06 to P = .49) and between days 4 and 7 at FE_{4mg} (P = .06 to P = .63). There was no difference in R2* change between non-MPS and LN R2* at any time (range, 1-71 sec^{-1} vs 0-50 sec^{-1}; P = .06 to P = .97). Conclusion The pharmacokinetics of ferumoxytol in lymph nodes are distinct from those in mononuclear phagocyte system (MPS) organs, parallel non-MPS anatomy, and the blood pool. © RSNA, 2019 Online supplemental material is available for this article.

DOI: https://doi.org/10.1148/radiol.2019190489

the Abdomen and Pelvis: A Dosing Study with 1.5- and 3.0-T MRI Relaxometry. Radiology, 294(1):108-116.
DOI: https://doi.org/10.1148/radiol.2019190489

Radiology

Pharmacokinetics of Ferumoxytol in the Abdomen and Pelvis: A Dosing Study with 1.5- and 3.0-T MRI Relaxometry

Shane A. Wells, MD • Tilman Schubert, MD • Utaroh Motosugi, MD, PhD • Samir D. Sharma, PhD • Camilo A. Campo, BS • Sonja Kinner, MD • Kaitlin M. Woo, MS • Diego Hernando, PhD • Scott B. Reeder, MD, PhD

Form the Departments of Radiology (S.A.W., T.S., U.M., S.D.S., C.A.C., S.K., D.H., S.B.R.), Biostatistics and Medical Informatics (K.M.W.), Biomedical Engineering (S.B.R.), Medical Physics (S.B.R.), Medicine (S.B.R.), and Emergency Medicine (S.B.R.), University of Wisconsin–Madison, University of Wisconsin School of Medicine and Public Health, 600 Highland Ave, E3/366, Madison, WI 53792; Clinic of Radiology and Nuclear Medicine, Basel University Hospital, Basel, Switzerland (T.S.); Department of Radiology, University of Yamanashi, Yamanashi, Japan (U.M.); and Department of Diagnostic and Interventional Radiology and Neuroradiology, University Hospital Essen, Germany (S.K.). Received March 2, 2019; revision requested May 6; revision received August 30; accepted September 30. **Address correspondence to** S.A.W. (e-mail: *sawells@wisc.edu*).

T.S. supported by a fellowship grant (Helmut-Hartweg-Fonds) from the Swiss Academy of Medical Sciences.

Conflicts of interest are listed at the end of this article.

Radiology 2020; 294:108–116 • https://doi.org/10.1148/radiol.2019190489 • Content codes: MI MR

Background: The off-label use of ferumoxytol (FE), an intravenous iron preparation for iron deficiency anemia, as a contrast agent for MRI is increasing; therefore, it is critical to understand its pharmacokinetics.

Purpose: To evaluate the pharmacokinetics of FE in the abdomen and pelvis, as assessed with quantitative 1.5- and 3.0-T MRI relaxometry.

Materials and Methods: R2*, an MRI technique used to estimate tissue iron content in the abdomen and pelvis, was performed at 1.5 and 3.0 T in 12 healthy volunteers between April 2015 and January 2016. Volunteers were randomly assigned to receive an FE dose of 2 mg per kilogram of body weight (FE_{2mg}) or 4 mg/kg (FE_{4mg}). MRI was repeated at 1.5 and 3.0 T for each volunteer at five time points: days 1, 2, 4, 7, and 30. A radiologist experienced in MRI relaxometry measured R2* in organs of the mononuclear phagocyte system (MPS) (ie, liver, spleen, and bone marrow), non-MPS anatomy (kidney, pancreas, and muscle), inguinal lymph nodes (LNs), and blood pool. A paired Student *t* test was used to compare changes in tissue R2*.

Results: Volunteers (six female; mean age, 44.3 years ± 12.2 [standard deviation]) received either $FE_{2\ mg}$ ($n = 5$) or $FE_{4\ mg}$ ($n = 6$). Overall R2* trend analysis was temporally significant ($P < .001$). Time to peak R2* in the MPS occurred on day 1 for FE_{2mg} and between days 1 and 4 for FE_{4mg} ($P < .001$ to $P < .002$). Time to peak R2* in non-MPS anatomy, LNs, and blood pool occurred on day 1 for both doses ($P < .001$ to $P < .09$). Except for the spleen (at 1.5 T) and liver, MPS R2* remained elevated through day 30 for both doses ($P = .02$ to $P = .03$). Except for the kidney and pancreas, non-MPS, LN, and blood pool R2* returned to baseline levels between days 2 and 4 at FE_{2mg} ($P = .06$ to $P = .49$) and between days 4 and 7 at FE_{4mg} ($P = .06$ to $P = .63$). There was no difference in R2* change between non-MPS and LN R2* at any time (range, 1–71 sec^{-1} vs 0–50 sec^{-1}; $P = .06$ to $P = .97$).

Conclusion: The pharmacokinetics of ferumoxytol in lymph nodes are distinct from those in mononuclear phagocyte system (MPS) organs, parallel non-MPS anatomy, and the blood pool.

Online supplemental material is available for this article.

Iron oxide nanoparticles, including ultrasmall superparamagnetic iron oxides (USPIOs), are gaining clinical interest as alternative MRI contrast agents. Similar to gadolinium-based contrast agents, USPIOs can be injected as a bolus, thereby allowing dynamic imaging of the aorta, mesenteric and renal arteries, and first-pass perfusion of the liver and kidneys (1). Because of slow migration (range, 12–14 hours) across the capillary endothelium, USPIOs are also useful as blood pool imaging agents for MR venography (2). Iron oxide nanoparticles, including USPIOs, are sequestered and cleared by the mononuclear phagocyte system (MPS) (3). While monocytes and macrophages of the MPS are in numerous tissues throughout the body, they are most abundant in the liver, spleen, and bone marrow, and to a lesser extent, the lymph nodes (LNs). As cells of the MPS accumulate USPIO, they progressively lose T2-weighted signal. Importantly, metastases, which lack macrophages, do not accumulate USPIO. Thus, hepatic metastases and LNs containing metastatic or micrometastatic disease can be identified by the lack of signal loss on T2-weighted MRI scans (4,5).

Ferumoxytol (FE) is an intravenous Food and Drug Administration–approved USPIO used to treat iron deficiency anemia in patients with chronic kidney disease (6). Because of favorable physical properties, FE is being used off-label as an MRI contrast agent where the safety profile (0.02%–1.3% rate of severe adverse events [hypersensitivity or hypotension]) is similar to that of ionic iodinated contrast agents (7,8). Unlike with gadolinium-based contrast agents that have renal and/or biliary excretion, the body has no active excretory pathway to dispose of excess iron from FE administration. Thus, it is critical to understand the pharmacokinetics of FE when it is used off-label, particularly when considering

Abbreviations

FE = ferumoxytol, FE_{2mg} = 2 mg/kg FE dose, FE_{4mg} = 4 mg/kg FE dose, LN = lymph node, MPS = mononuclear phagocyte system, ROI = region of interest, USPIO = ultrasmall superparamagnetic iron oxide

Summary

The 30-day pharmacokinetics of ferumoxytol in organs of the mononuclear phagocyte system are distinct from those in organs such as the kidney, pancreas, and muscle; the pharmacokinetics of ferumoxytol in inguinal lymph nodes mirror those of the blood pool.

Key Results

- After infusion of ferumoxytol, liver and spleen R2* peaked on days 1 and 2, respectively.
- Liver and spleen R2* returned to baseline level by day 30 after infusion of 2 mg/kg ferumoxytol but remained elevated after infusion of 4 mg/kg ferumoxytol.
- Peak R2* of kidney, pancreas, muscle, inguinal lymph nodes, and blood pool occurred 1 day after administration of both 2mg/kg and 4mg/kg of ferumoxytol.
- Similar to blood pool, clearance of ferumoxytol from kidney, pancreas, muscle and inguinal lymph nodes occurred on day 2 for 2mg/kg and day 4 for 4mg/kg at both 1.5 T and 3.0 T.

repeat administration for cancer staging and restaging. To our knowledge, the optimal dose, time to peak tissue concentration, and clearance from the organs of the MPS are unknown to date. Thus, the purpose of our study was to evaluate the pharmacokinetics of FE in the abdomen and pelvis, as assessed with quantitative MRI relaxometry at 1.5 and 3.0 T. We hypothesize that *(a)* the time to peak tissue concentration and clearance of FE for the mononuclear phagocyte system (MPS) and non-MPS will differ and *(b)* peak tissue concentration and clearance of FE from the inguinal LNs, non-MPS, and blood pool will be similar.

Materials and Methods

Study Volunteers

Our prospective randomized clinical trial was compliant with the Health Insurance Portability and Accountability Act (HIPAA) and was approved by our local institutional review board (IRB). Twelve healthy volunteers were recruited from a local IRB-approved HIPAA-compliant database. Volunteers younger than 18 years were excluded. Volunteers signed written informed consent.

Study Protocol

The study consisted of six visits over 4 weeks for each volunteer from April 2015 to January 2016. Eleven volunteers were imaged with noncontrast MRI at 1.5 and 3.0 T at each visit.

At visit 1 (day 0), noncontrast 1.5- and 3.0-T MRI examinations of the abdomen and pelvis were performed in all volunteers to establish baseline R2*; this is an MRI technique used to estimate tissue iron content.

Volunteers were randomly assigned to receive a dose of 2 mg FE per kilogram of body weight (FE_{2mg}) (0.035 mmol FE per kilogram, $n = 6$) or 4 mg FE per kilogram of body weight (FE_{4mg}) (0.07 mmol FE per kilogram, $n = 6$). The FE (Feraheme; AMAG Pharmaceuticals, Waltham, Mass) doses in our study were chosen based on guidelines and doses used in the literature (9,10).

Injection parameters followed International Society for Magnetic Resonance in Medicine guidelines (9). Doses were diluted to 60 mL (saline) and were administered intravenously via bolus injection at a rate of 2 mL/sec (Spectris Solaris; MedRAD, Warrendale, Pa) and were followed by a 20-mL saline flush. Bolus injection was performed as part of a companion study evaluating first-pass MR angiography (1). Volunteers' vital signs were recorded prior to, during, and 15 and 60 minutes after FE administration. Volunteers were evaluated for hypersensitivity reactions at discharge.

For visits 2, 3, 4, 5, and 6, volunteers returned on days 1, 2, 4, 7, and 30 after FE administration for 1.5- and 3.0-T MRI of the abdomen and pelvis. The imaging interval was designed to explore peak R2* and clearance of FE from the blood pool and MPS organs compared with non-MPS anatomy and LNs. Figure 1 shows an overview of the study protocol.

MRI Protocol

MRI was performed at 1.5 T (HDxt; GE Healthcare, Waukesha, Wis) and 3.0 T (MR750; GE Healthcare) using an eight-channel phased-array body coil at 1.5 T (USA Instruments/GE Healthcare, Waukesha, Wis) or a 32-channel phased-array body coil at 3.0 T (Neocoil, Pewaukee, Wis). The MRI protocol included quantitative R2* mapping based on a chemical shift–encoded multiecho three-dimensional spoiled gradient-echo pulse sequence.

Imaging parameters for chemical shift–encoded 1.5-T MRI were as follows: In the abdomen, axial acquisition was performed (repetition time msec/echo time msec, 15.5/1.24; ΔTE = 1.72 msec; six echoes per repetition time; 256 × 160 × 32 matrix; 400 × 360 mm field of view; 8.0-mm section thickness for a true spatial resolution of 1.6 × 2.3 × 8.0 mm; 5° flip angle; receiver bandwidth, ±62.5 kHz). In the pelvis, axial acquisition was performed (15.5/1.24, ΔTE = 1.72 msec; six echoes per repetition time; 256 × 160 × 80 matrix; 400 × 360 mm field of view; 3.0-mm slice thickness; true spatial resolution, 1.6 × 2.3 × 3.0 mm; 12° flip angle; ±62.5 kHz receiver bandwidth).

Imaging parameters for chemical shift–encoded 3.0-T MRI were as follows: In the abdomen, axial acquisition was performed (8.0/1.24; ΔTE = 1.01 msec; six echoes were obtained by interleaving two echo trains of three echoes over two repetition times; 256 × 144 × 28 matrix, 400 × 360 mm field of view; 8-mm slice thickness for a true spatial resolution of 1.6 × 2.8 × 8.0 mm; 4° flip angle; receiver bandwidth, ±125 kHz). In the pelvis, axial acquisition was performed (8.0/1.24; ΔTE, 1.01 msec; six echoes were obtained by interleaving two echo trains of three echoes over two repetition times; matrix, 256 × 160 × 80; 400 × 360 mm field of view; 3-mm slice thickness for a true spatial resolution of 1.6 × 2.8 × 3.0 mm; flip angle, 9°; receiver bandwidth, ±125 Hz).

R2* Measurements

The chemical shift–encoded MRI data were processed by using a confounder-corrected R2* mapping algorithm that corrects

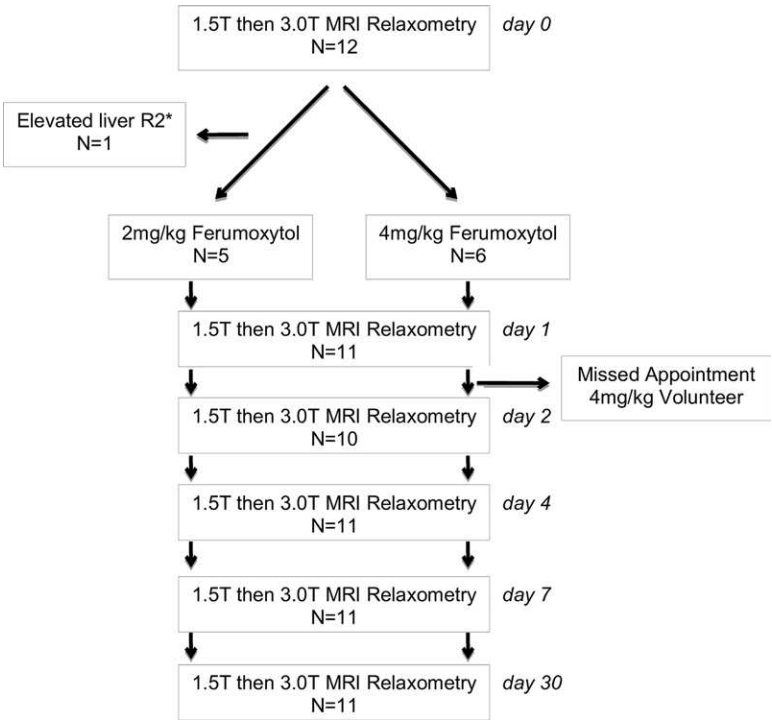

Figure 1: Study protocol diagram.

for the effects of fat and noise floor (11,12). R2* was measured by drawing two elliptical regions of interest (ROIs) on the liver (right and left lobes), spleen, kidney (cortex and medulla), inferior vena cava, and lumbar (L2) and thoracic (T12) vertebral bodies (marrow), and one ROI on the pancreas, aorta, erector spinae muscle, and right and left inguinal lymph nodes. ROIs were drawn as large as possible to fit within the parenchyma of the specified organ, avoiding structures (eg, large blood vessels, bile ducts) and obvious image artifacts. ROIs were placed independently by a board-certified radiologist (T.S., 9 years of experience in abdomen and pelvis MRI).

Statistical Analysis

R2* values were quantified at each visit for each dose at 1.5 and 3.0 T. For anatomy with more than one ROI, measurements were averaged at each time point for each volunteer.

Linear trend analysis for all R2* measurements as a function of time was performed. MPS organs (liver, spleen, and bone marrow), non-MPS anatomy (kidney, pancreas, and muscle), and blood pool (aorta and inferior vena cava) were stratified. ROI measurements were averaged for blood pool and for each system at each time point for each volunteer. These stratified averages were used for subsequent analysis. Median and interquartile range are presented as summary statistics.

A paired Student *t* test was used to *(a)* evaluate change in organ, anatomy, and LN R2* from baseline, defined as contrast material–enhanced R2* minus noncontrast R2* and *(b)* compare LN R2* with non-MPS anatomy R2*.

Statistical tests were two sided, and 5% ($P < .05$) was set as the level of significance. Statistical analysis was performed with open-source software (R, version 3.3.1; R Foundation, Vienna, Austria).

Results

Eleven volunteers completed the study protocol (six female; mean age, 44.3 years ± 12.2 [standard deviation]; mean body mass index, 29.1 ± 5.5). One male volunteer had elevated liver R2* at baseline and was therefore excluded from the analysis. Five volunteers received FE_{2mg}, and six volunteers received FE_{4mg}. All imaging examinations except one (day 2, FE_{4mg}) were completed successfully. The overall R2* trend analysis was temporally significant ($P < .001$). No adverse events were observed.

Figure 2 shows quantitative R2* maps in the abdomen of two volunteers acquired over the six visits after FE_{2mg} and FE_{4mg} at 1.5 T. Figure 3 shows quantitative R2* maps in the pelvis of two volunteers acquired with FE_{2mg} and FE_{4mg} at 1.5 T. The pharmacokinetics of FE can be observed qualitatively over the 30-day period for the MPS compared with inguinal LNs.

Inguinal Lymph Node R2*

Figures 4–6 compare LN R2* with MPS organ, non-MPS anatomy, and blood pool R2* before and after administration of FE_{2mg} and FE_{4mg} at 1.5 and 3.0 T.

For FE_{2mg}, LN R2* increased and peaked on day 1 at 1.5 T (27 sec^{-1} vs 39 sec^{-1}, $P = .01$) and was similar to baseline R2* by day 2 (28 sec^{-1}, $P = .09$). LN R2* did not change at 3.0 T ($P = .06$ to $P = .42$).

For FE_{4mg}, LN R2* increased and peaked on day 1 at 1.5 T (18 sec^{-1} vs 91 sec^{-1}, $P = .003$) and 3.0 T (51 sec^{-1} vs 16 sec^{-1}, $P = .002$). LN R2* was similar to that at baseline by day 4 at 1.5 T (30 sec^{-1}, $P = .07$) and by day 7 at 3.0 T (52 sec^{-1}, $P = .24$).

For FE_{2mg}, there was no significant difference in change of R2* between LN and non-MPS anatomy ($P = .1$ for $P = 0.97$). The median R2* change in LN ranged from 1 to 15 sec^{-1} at 1.5 T and from 1 to 11 sec^{-1} at 3.0 T, while the median R2* change in non-MPS anatomy ranged from 0 to 14 sec^{-1} at 1.5 and 3.0 T.

For FE_{4mg}, there was also no significant difference in change of R2* between LN and non-MPS anatomy ($P = .06$ to $P = .76$). The median R2* change in LN ranged from 1 to 71 sec^{-1} at 1.5 T and from 3 to 67 sec^{-1} at 3.0 T, while the median R2* change in non-MPS anatomy ranged from 0 to 50 sec^{-1} at 1.5 T and from 0 to 46 sec^{-1} at 3.0 T.

R2* and change of R2* between LN and non-MPS anatomy at baseline and across visits is summarized in Table 1 for 1.5-T imaging and in Table 2 for 3.0-T imaging.

MPS Organ R2*

At FE_{2mg}, R2* increased in the MPS organs (liver, spleen, and bone marrow, respectively) on day 1 at both 1.5 T (27 sec^{-1} vs 126 sec^{-1}, 9 sec^{-1} vs 214 sec^{-1}, and 57 sec^{-1} vs 231 sec^{-1}; $P < .001$) and 3.0 T (41 sec^{-1} vs 148 sec^{-1}, 17 sec^{-1} vs 230 sec^{-1}, and 138 sec^{-1} vs 321 sec^{-1}; $P < .001$) and continued through day 7 (1.5 T: 45, 45, and 111 sec^{-1}; 3.0 T: 61, 62, and 199

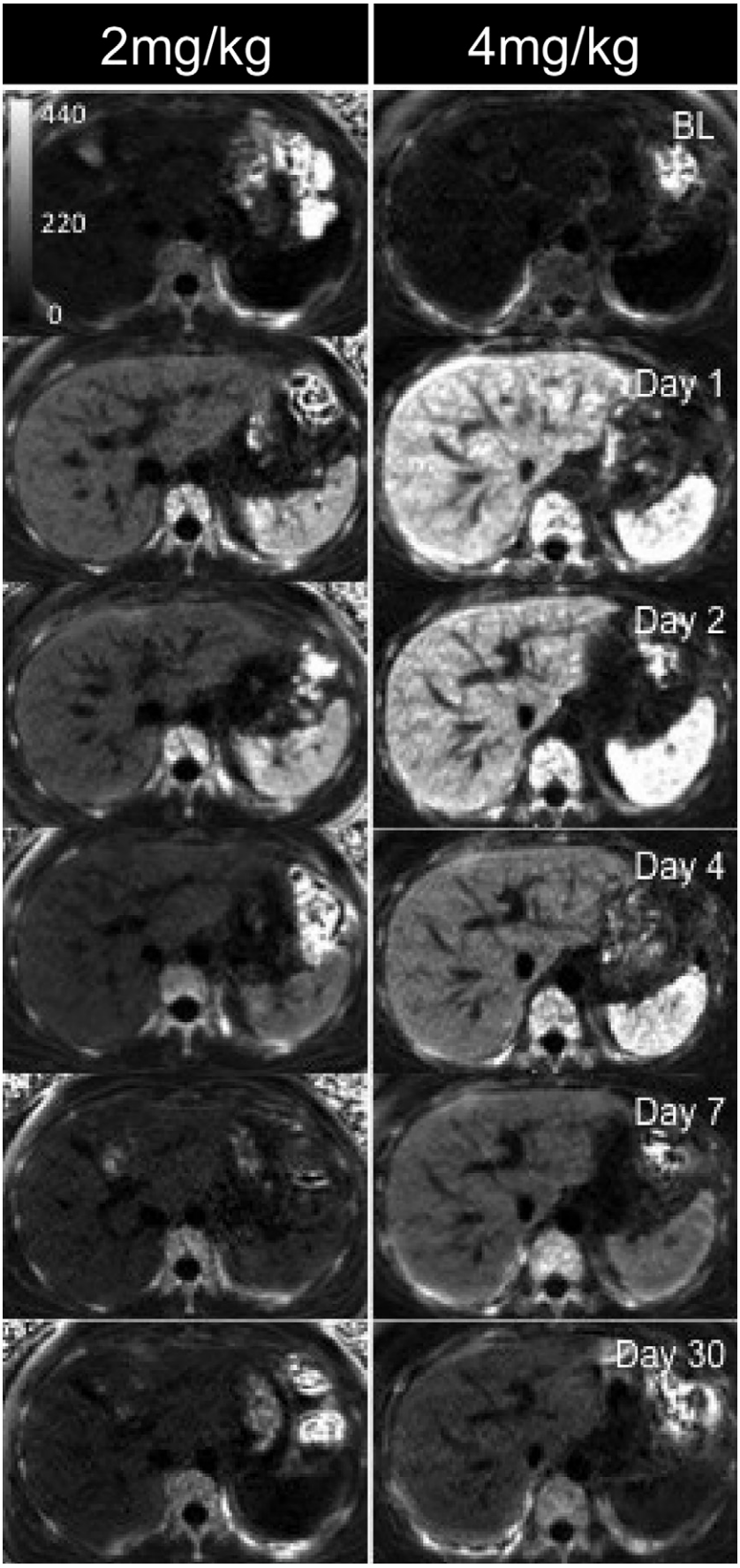

Figure 2: R2* maps of the abdomen in a volunteer who received 2 mg/kg ferumoxytol (FE) (left) and a volunteer who received 4 mg/kg FE (right) show biodistribution and clearance of FE in mononuclear phagocyte system organs (liver, spleen, and bone marrow) at 1.5-T MRI at baseline (BL) and across visits (days 1, 2, 4, 7, and 30). Window level was set to 220 sec^{-1}, and window width was set to 440 sec^{-1} for all images.

sec^{-1}; $P < .01$). Similarly, after injection of FE_{4mg}, R2* increased in the MPS organs on day 1 at both 1.5 T (44 sec^{-1} vs 293 sec^{-1}, 22 sec^{-1} vs 360 sec^{-1}, and 80 sec^{-1} vs 337 sec^{-1}; $P < .001$) and 3.0 T (81 sec^{-1} vs 319 sec^{-1}, 37 sec^{-1} vs 416 sec^{-1}, and 218 sec^{-1} vs 406 sec^{-1}; $P < .001$) and continued through day 30 (1.5 T: 100, 67, and 140 sec^{-1}; 3.0 T: 153, 101, and 352 sec^{-1}; $P < .02$).

Time to peak R2* in the liver, spleen, and bone marrow occurred on day 1 for FE_{2mg} at 1.5 and 3.0 T. However, time to peak R2* varied by organ and field strength for FE_{4mg}. Liver R2* peaked on day 1 at both 1.5 and 3.0 T, while spleen R2* peaked on day 2. Bone marrow R2* peaked on day 2 at 1.5 T and on day 4 at 3.0 T.

On day 30 for FE_{2mg}, liver R2* was similar to baseline R2* at 1.5 T (30 sec^{-1}, $P = .1$) and 3.0 T (41 sec^{-1}, $P = .76$). Spleen R2* was similar to baseline R2* at 1.5 T (15 sec^{-1}, $P = .13$) but remained higher than baseline R2* at 3.0 T (22 sec^{-1}, $P = .02$). Bone marrow R2* remained higher than baseline R2* at both field strengths (1.5 T: 86 sec^{-1}, $P = .02$; 3.0 T: 168 sec^{-1}, $P = .03$).

On day 30 for FE_{4mg}, liver, spleen, and bone marrow R2* remained higher than baseline R2* at both field strengths (1.5 T: 100, 67, and 140 sec^{-1}, respectively; 3.0 T: 153, 101, and 352 sec^{-1}, respectively; $P < .04$). R2* of MPS organs at baseline and across visits is summarized in Tables E1 and E2 (online).

Non-MPS Anatomy R2*

For FE_{2mg}, R2* increased and peaked in the blood pool, kidney, and pancreas on day 1 (5 sec^{-1} vs 28 sec^{-1}, 13 sec^{-1} vs 31 sec^{-1}, 19 sec^{-1} vs 35 sec^{-1}, respectively; $P < .01$). On day 2, only the R2* of blood pool at 1.5 T remained higher than that at baseline (12 sec^{-1}, $P = .02$). By day 4, the R2* of blood pool at 1.5 T was similar to that at baseline (8 sec^{-1}, $P = .13$). Muscle did not demonstrate a change in R2*.

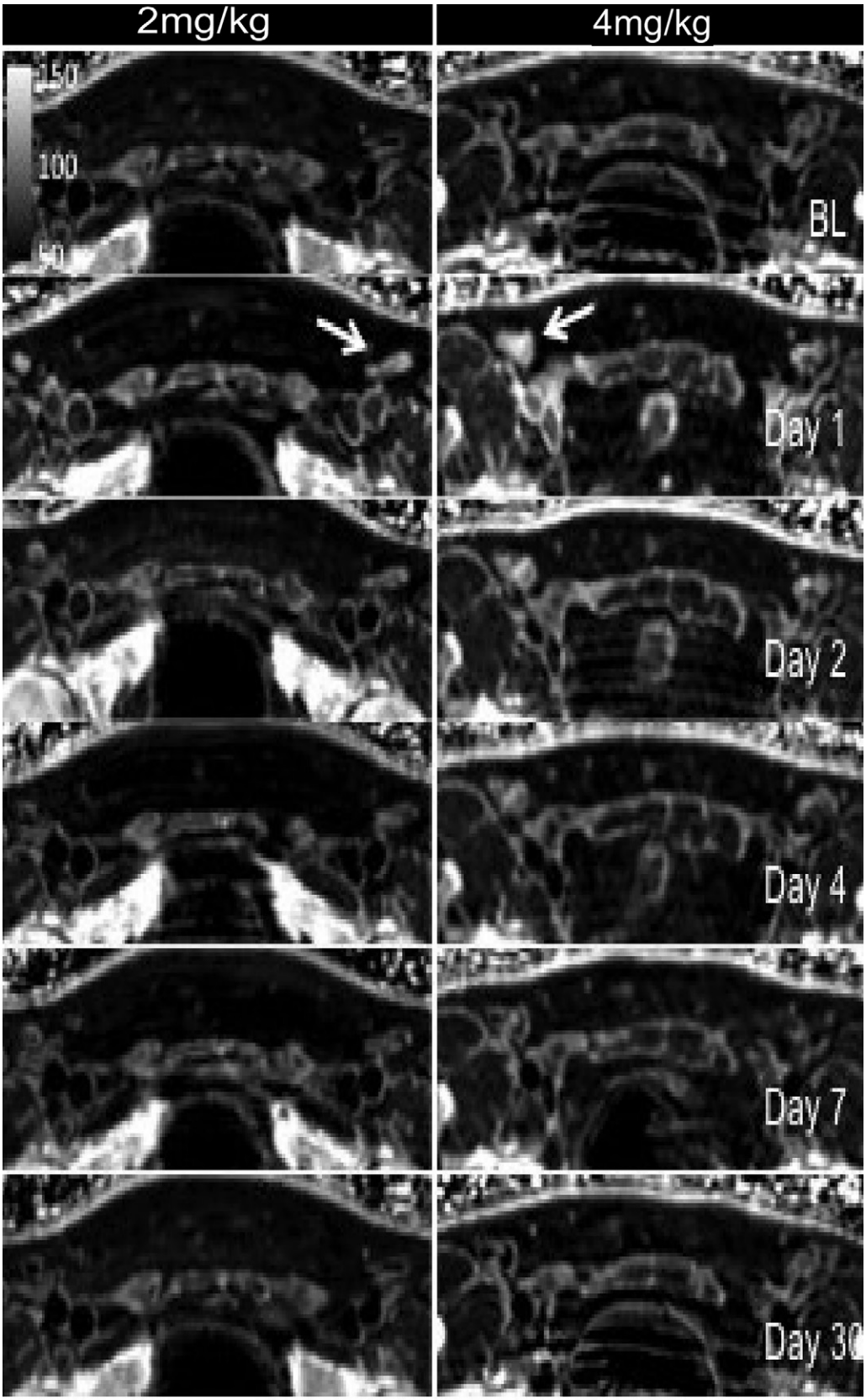

Figure 3: R2* maps of the pelvis in a volunteer who received 2 mg/kg ferumoxytol (FE) (left) and a volunteer who received 4 mg/kg FE (right) show the biodistribution and clearance of FE in inguinal lymph nodes (arrows) at 1.5-T MRI at baseline (BL) and across visits (days 1, 2, 4, 7, and 30). Window level was set to 220 sec^{-1}, and window width was set to 440 sec^{-1} for all images.

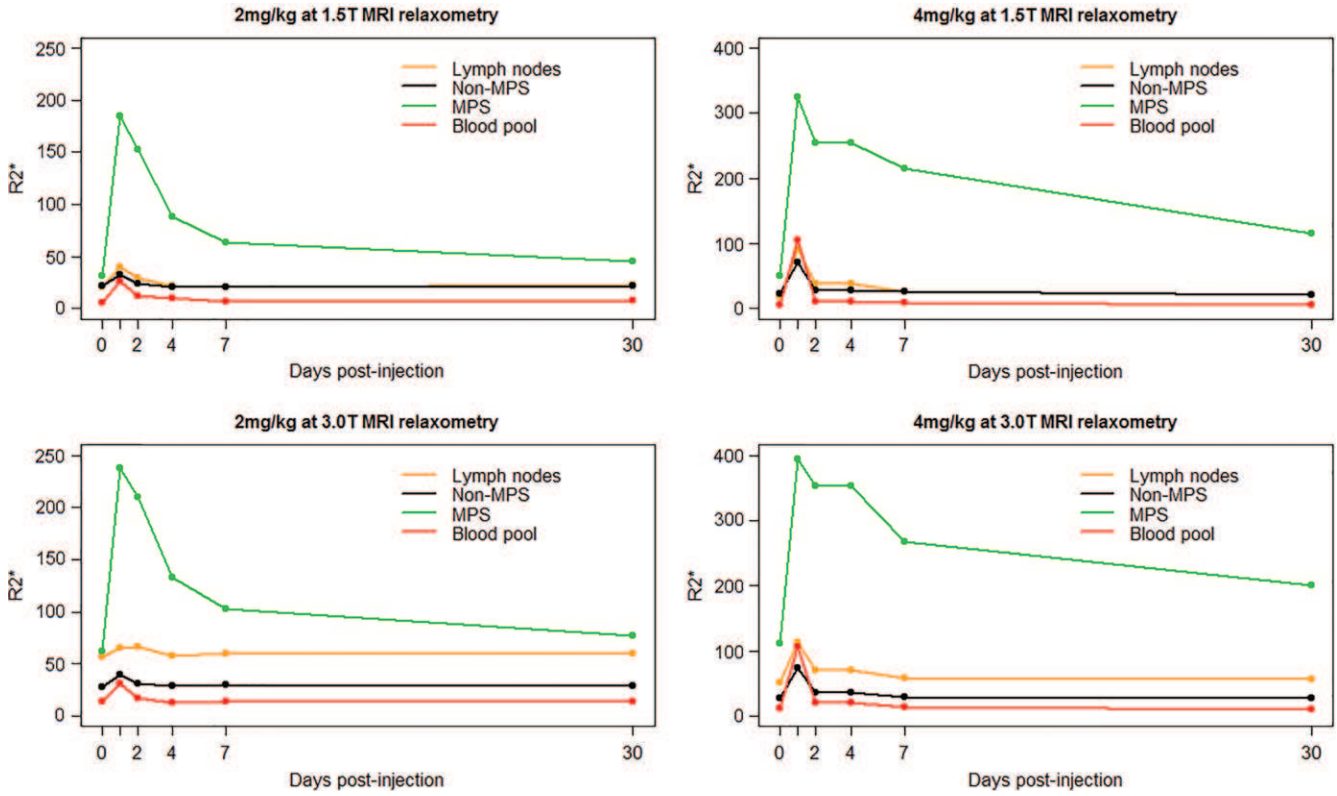

Figure 4: Graphs show pharmacokinetics of ferumoxytol (FE) in the mononuclear phagocyte system (MPS) organs (liver, spleen, and bone marrow), non-MPS anatomy (kidney, pancreas, and muscle), blood pool (aorta and inferior vena cava), and inguinal lymph nodes across visits (days 0, 1, 2, 4, 7, and 30). Left: Pharmacokinetics of 2 mg/kg FE at 1.5- (top) and 3.0-T (bottom) MRI. Right: Pharmacokinetics of 4 mg/kg of FE at 1.5- (top) and 3.0-T (bottom) MRI.

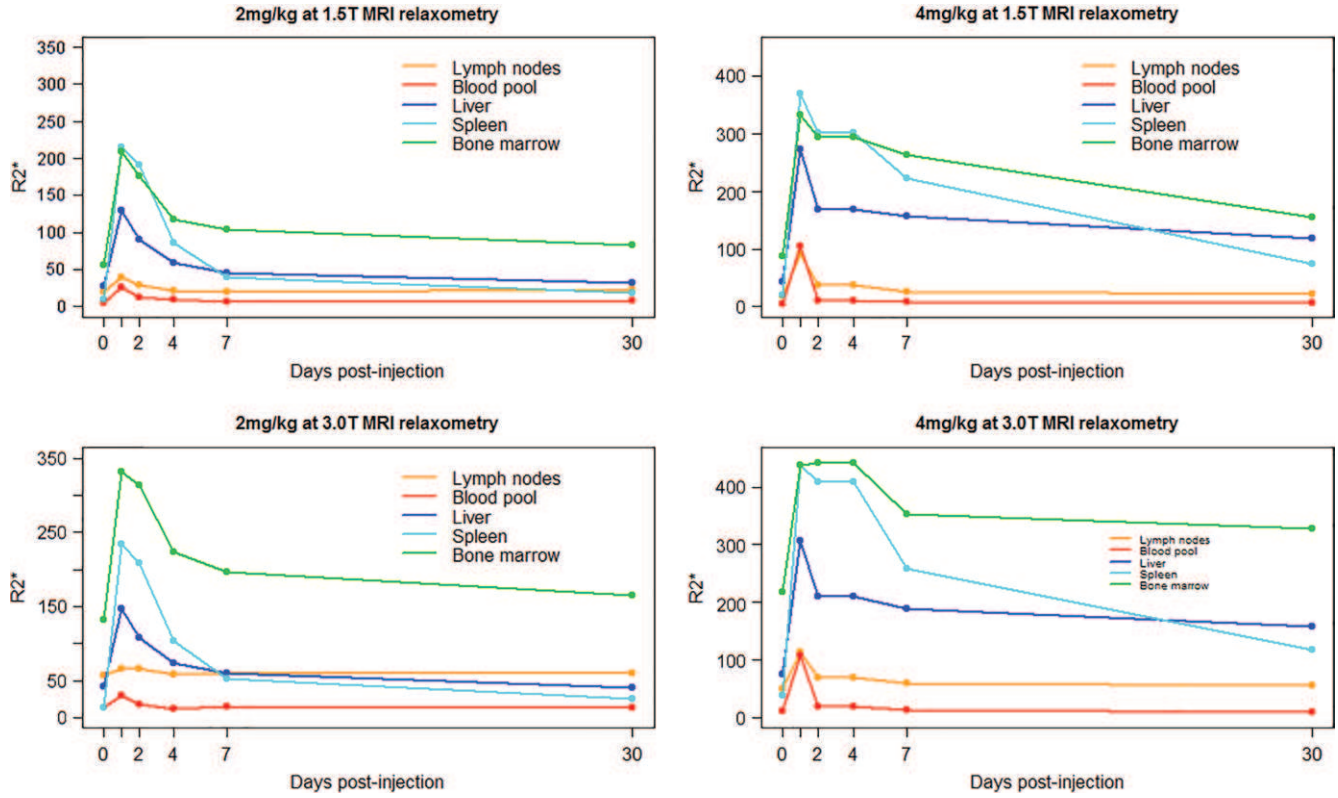

Figure 5: Graphs show pharmacokinetics of ferumoxytol (FE) in the mononuclear phagocyte organs (liver, spleen, and bone marrow), blood pool (aorta and inferior vena cava), and inguinal lymph nodes across visits (days 0, 1, 2, 4, 7, and 30). Left: Pharmacokinetics of 2 mg/kg FE at 1.5- (top) and 3.0-T (bottom) MRI. Right: Pharmacokinetics of 4 mg/kg FE at 1.5- (top) and 3.0-T (bottom) MRI.

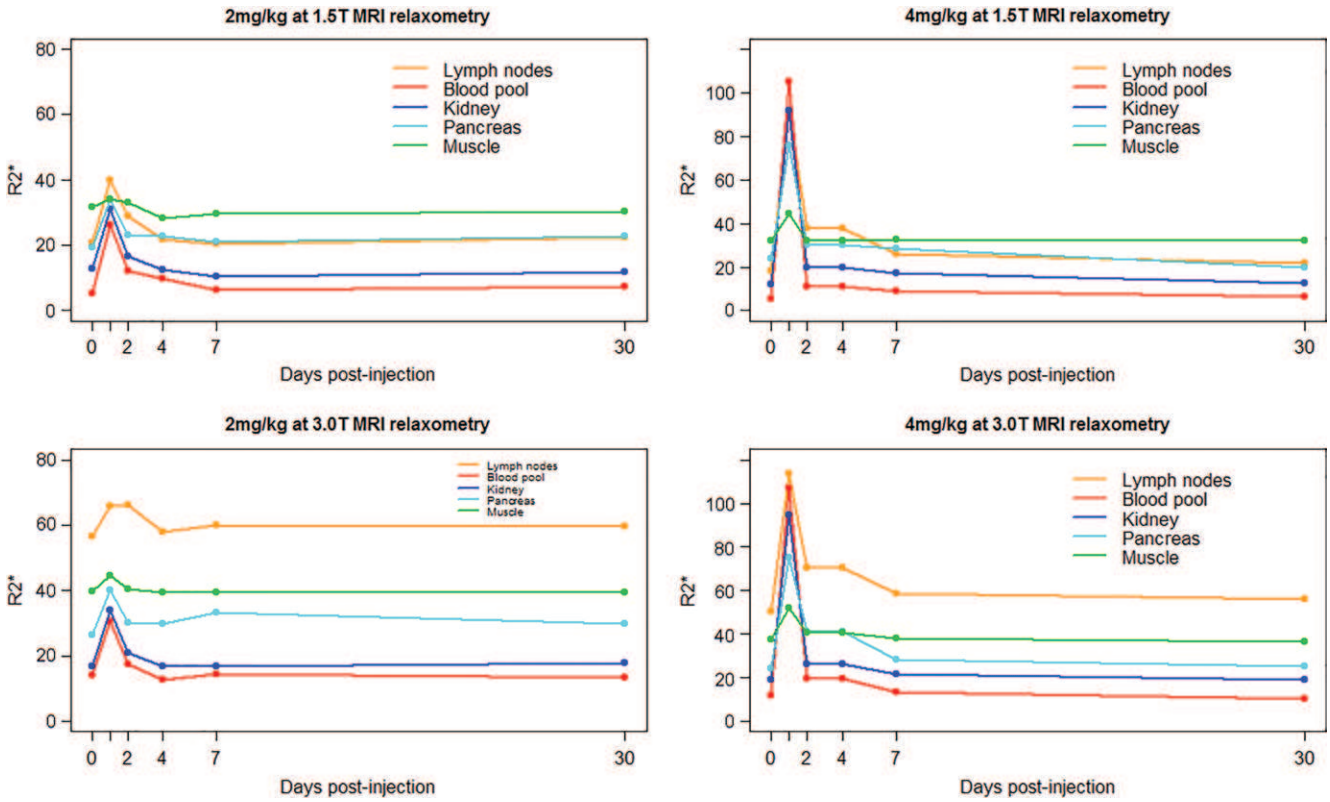

Figure 6: Graphs show pharmacokinetics of ferumoxytol (FE) in the non–mononuclear phagocyte system anatomy (kidney, pancreas, and erector spinae muscle), blood pool (aorta and inferior vena cava), and inguinal lymph nodes across visits (days 0, 1, 2, 4, 7, and 30). Left: Pharmacokinetics of 2 mg/kg FE at 1.5- (top) and 3.0-T (bottom) MRI. Right: Pharmacokinetics of 4 mg/kg FE at 1.5- (top) and 3.0-T (bottom) MRI.

Table 1: Inguinal LN and Non-MPS Anatomy R2* Values at 1.5-T MRI at Baseline and across Visits after Intravenous Administration of Ferumoxytol

Time Point	LN R2*	Non-MPS R2*	*P* Value	LN R2* Change	Non-MPS R2* Change	*P* Value
	Ferumoxytol 2 mg/kg at 1.5-T MRI Relaxometry					
Baseline	21 (17–24)	17 (16–18)	.18	…	…	…
Day 1	39 (37–41)	33 (30–33)	.003	15 (13–24)	14 (13–17)	.11
Day 2	29 (28–29)	21 (21–22)	.003	8 (5–11)	3 (3–6)	.23
Day 4	25 (20–28)	17 (17–18)	.37	2 (1–7)	1 (0–2)	.96
Day 7	19 (18–25)	17 (16–18)	.36	1 (0–5)	0 (0–1)	.97
Day 30	22 (21–25)	18 (16–19)	.08	3 (0–5)	1 (0–1)	.59
	Ferumoxytol 4 mg/kg at 1.5-T MRI Relaxometry					
Baseline	18 (17–20)	18 (17–19)	.94	…	…	…
Day 1	91 (63–111)	68 (66–91)	.45	71 (47–93)	50 (47–72)	.45
Day 2	41 (40–78)	36 (35–39)	.5	26 (20–60)	19 (18–19)	.5
Day 4	30 (23–48)	23 (20–27)	.11	13 (4–30)	3 (2–8)	.12
Day 7	23 (20–33)	21 (21–24)	.21	2 (2–16)	4 (2–6)	.24
Day 30	21 (19–25)	17 (16–19)	.08	1 (0–8)	0 (0–1)	.13

Note.—Data are the median, and data in parentheses are the interquartile range. LN = inguinal lymph node, MPS = mononuclear phagocyte system.

For FE_{4mg}, R2* of blood pool and non-MPS anatomy, including muscle, increased and peaked on day 1 (5 sec^{-1} vs 87 sec^{-1} [blood pool], 12 sec^{-1} vs 83 sec^{-1} [kidney], 23 sec^{-1} vs 67 sec^{-1} [pancreas], and 32 sec^{-1} vs 44 sec^{-1} [muscle]; $P < .001$). By day 4, R2* of the blood pool and non-MPS anatomy, except for the pancreas at 3.0 T (25 sec^{-1} vs 40 sec^{-1}, $P = .04$) and the kidney at 1.5 T (12 sec^{-1} vs 19 sec^{-1}, $P = .02$), were similar to those at baseline. R2* of the pancreas and kidney were similar to baseline values by day 7. The R2* values of blood pool and non-MPS anatomy at baseline and across visits are summarized in Tables E1 and E2 (online).

Table 2: Inguinal Lymph Node and Non–Mononuclear Phagocyte System Anatomy R2* Values at 3.0-T MRI at Baseline and across Visits after Intravenous Administration of Ferumoxytol

Time Point	LN R2*	Non-MPS R2*	*P* Value	LN R2* Change	Non-MPS R2* Change	*P* Value
	Ferumoxytol 2 mg/kg at 3.0-T MRI Relaxometry					
Baseline	54 (52–60)	25 (22–25)	<.001	…	…	…
Day 1	67 (63–68)	38 (38–40)	.002	11 (7–14)	14 (13–15)	.46
Day 2	62 (62–74)	27 (24–30)	<.001	8 (6–9)	3 (2–4)	.1
Day 4	57 (53–63)	24 (24–26)	<.001	1 (0–4)	0 (0–1)	.68
Day 7	60 (55–64)	25 (28–29)	<.001	4 (3–4)	0 (0–1)	.58
Day 30	60 (55–64)	24 (22–30)	<.001	3 (0–7)	0 (0–1)	.44
	Ferumoxytol 4 mg/kg at 3.0-T MRI Relaxometry					
Baseline	51 (49–53)	22 (21–25)	<.001	…	…	…
Day 1	116 (94–129)	69 (68–95)	.04	67 (42–81)	46 (43–74)	.76
Day 2	76 (74–94)	42 (37–47)	.01	23 (17–53)	21 (15–21)	.4
Day 4	63 (61–75)	32 (29–35)	.001	17 (8–27)	10 (5–11)	.19
Day 7	52 (49–68)	25 (24–26)	.002	3 (0–21)	2 (0–4)	.39
Day 30	56 (54–59)	23 (22–23)	<.001	7 (3–8)	0 (0–0)	.06

Note.—Data are the median, and data in parentheses are the interquartile range. LN = inguinal lymph node, MPS = mononuclear phagocyte system.

Discussion

Ferumoxytol (FE), an ultrasmall superparamagnetic iron oxide (USPIO) used to treat iron deficiency anemia in the setting of chronic kidney disease, is being increasingly used off-label as a contrast agent for MRI. Because the body has no active excretory pathway to dispose of excess iron, it is critical to understand the pharmacokinetics of FE. We evaluated the pharmacokinetics of FE at two doses, FE_{2mg} and FE_{4mg}, in the abdomen and pelvis with 1.5- and 3.0-T MRI relaxometry. As expected, the pharmacokinetics of FE in the mononuclear phagocyte system (MPS), which includes the liver, spleen, and bone marrow, are distinct from the pharmacokinetics of FE in the blood pool and non-MPS anatomy, including the kidney, pancreas, and muscle. MPS R2* remained elevated through day 30 for both doses (except for the liver and spleen at 1.5 T and with FE_{2mg}) while non-MPS anatomy returned to baseline by day 2 with FE_{2mg} (except blood pool) and by day 4 with $FE4_{mg}$ (except pancreas and muscle). Peak R2* of MPS organs was organ specific and dose dependent. R2* peaked in the liver, spleen, and bone marrow on day 1 at 1.5 and 3.0 T after FE_{2mg}. At FE_{4mg}, R2* peaked in the liver on day 1 and in the spleen on day 2 (at both field strengths), while bone marrow R2* peaked on day 2 at 1.5 T and on day 4 at 3.0 T. The pharmacokinetics of FE in the inguinal lymph nodes paralleled blood pool and non-MPS anatomy. Similar to blood pool and non-MPS organ R2*, inguinal lymph node R2* peaked on day 1 and returned to the baseline level on day 2 for FE_{2mg} and on days 4 (1.5 T) and 7 (3.0 T) for FE_{4mg}.

The premise of using USPIO to detect metastatic disease depends on prolonged uptake in macrophages in lymph nodes and organs of the MPS. Unlike MPS organs, inguinal lymph nodes do not demonstrate prolonged uptake of FE. Therefore, both normal lymph nodes and lymph nodes harboring metastatic disease would appear similar with MRI relaxometry. Our results support a recent phase I MR lymphography dosing study of 15 patients with prostate cancer (13). Turkbey et al (13) found that inguinal lymph node signal loss was heterogeneous and could result in false-positive diagnosis with 4, 6, or 7.5 mg/kg doses when imaged at 3.0 T 1 day after FE administration. In 2008, the European Medicines Agency, which is the European equivalent of the Food and Drug Administration, declined to approve the use of ferumoxtran 10 (Sinerem; Guerbet, Villepinte, France), a USPIO with a similar particle size as FE (mean diameter, 30 nm), for MR lymphography (14). They cited, among other studies, an unpublished randomized multicenter open-label trial that enrolled 271 patients with pelvic cancer (prostate, bladder, uterine, or cervix cancer) who underwent MRI and MR lymphography (dose, 2.6 mg/kg) prior to lymphadenectomy. They found that MR lymphography lacked sensitivity, failed noninferiority for specificity, and demonstrated a lack of consistency among the three study radiologists. While the European Medicines Agency cited an increase in sensitivity, they concluded that a reduction in specificity might confound the potential therapeutic benefit for MR lymphography.

Our study adds to the growing body of literature demonstrating the excellent safety profile of intravenous FE when used with MRI. Similar to other recent MRI and MR lymphography studies (13,15–17), there were no serious adverse events in our study. Large cohort studies in patients with iron deficiency anemia from chronic kidney disease (n = 9820) found that the rate of serious adverse events (range, 0%–1%) and anaphylaxis (0.03%) was similar to those of ionic iodinated contrast agents (18–22). Importantly, the rate of serious adverse events may be even lower in imaging studies where the FE dose is, in general, substantially lower than the therapeutic doses (9). By diluting FE and reducing the rate of intravenous administration over 15 minutes, as recommended by the Food and Drug Administration, one may further mitigate the risk of serious adverse events.

Our study had several limitations. Our study design with two doses and imaging at both 1.5 and 3.0 T are study strengths, but this created two relatively small groups. As a result, our study was underpowered to detect small differences in R2*, which likely explains the discrepancy in time to organ-specific peak R2* between field strengths. On the basis of the calculated residual errors, the between-group mean difference in R2* would need to be at least 40.1 sec^{-1} for 80% power. Because our study was performed in healthy volunteers, we used non-MPS tissues as a tumor surrogate. Similar to metastases, non-MPS tissues do not contain tissue macrophages and do not accumulate USPIO. Therefore, we believe that the pharmacokinetics of FE in non-MPS tissues should approximate metastases where perfusion is the primary source of signal change.

In conclusion, we found that peak R2* and maximum signal change in tissues of the mononuclear phagocyte system (MPS) are organ specific and dose dependent. At higher ferumoxytol (FE) doses, biodistribution is constant but clearance is prolonged, with bone marrow likely representing the dose-limiting organ. The pharmacokinetics of FE in inguinal lymph nodes closely parallel blood pool and non-MPS anatomy. Therefore, FE likely has little utility in detecting metastatic disease to these lymph nodes.

Author contributions: Guarantors of integrity of entire study, S.A.W., S.B.R.; study concepts/study design or data acquisition or data analysis/interpretation, all authors; manuscript drafting or manuscript revision for important intellectual content, all authors; approval of final version of submitted manuscript, all authors; agrees to ensure any questions related to the work are appropriately resolved, all authors; literature research, S.A.W., T.S., U.M., C.A.C., S.K., D.H., S.B.R.; clinical studies, S.A.W., T.S., U.M., C.A.C., S.K.; statistical analysis, S.A.W., T.S., K.M.W., S.B.R.; and manuscript editing, S.A.W., T.S., S.D.S., C.A.C., S.K., K.M.W., D.H., S.B.R.

Disclosures of Conflicts of Interest: S.A.W. Activities related to the present article: disclosed no relevant relationships. Activities not related to the present article: is an educational consultant for Ethicon. Other relationships: disclosed no relevant relationships. **T.S.** disclosed no relevant relationships. **U.M.** Activities related to the present article: disclosed no relevant relationships. Activities not related to the present article: received research support from GE Healthcare and Bayer Healthcare. Other relationships: disclosed no relevant relationships. **S.D.S.** disclosed no relevant relationships. **C.A.C.** disclosed no relevant relationships. **S.K.** disclosed no relevant relationships. **K.M.W.** disclosed no relevant relationships. **D.H.** Activities related to the present article: disclosed no relevant relationships. Activities not related to the present article: is a cofounder of Calimetrix. Other relationships: disclosed no relevant relationships. **S.B.R.** disclosed no relevant relationships.

References

1. Schubert T, Motosugi U, Kinner S, et al. Crossover comparison of ferumoxytol and gadobenate dimeglumine for abdominal MR-angiography at 3.0 tesla: Effects of contrast bolus length and flip angle. J Magn Reson Imaging 2017;45(6):1617–1626.
2. Han F, Rapacchi S, Khan S, et al. Four-dimensional, multiphase, steady-state imaging with contrast enhancement (MUSIC) in the heart: a feasibility study in children. Magn Reson Med 2015;74(4):1042–1049.
3. Storey P, Lim RP, Chandarana H, et al. MRI assessment of hepatic iron clearance rates after USPIO administration in healthy adults. Invest Radiol 2012;47(12):717–724.
4. Toth GB, Varallyay CG, Horvath A, et al. Current and potential imaging applications of ferumoxytol for magnetic resonance imaging. Kidney Int 2017;92(1):47–66.
5. McDermott S, Thayer SP, Fernandez-Del Castillo C, Mino-Kenudson M, Weissleder R, Harisinghani MG. Accurate prediction of nodal status in preoperative patients with pancreatic ductal adenocarcinoma using next-gen nanoparticle. Transl Oncol 2013;6(6):670–675.
6. Spinowitz BS, Kausz AT, Baptista J, et al. Ferumoxytol for treating iron deficiency anemia in CKD. J Am Soc Nephrol 2008;19(8):1599–1605.
7. Knobloch G, Colgan T, Wiens CN, et al. Relaxivity of Ferumoxytol at 1.5 T and 3.0 T. Invest Radiol 2018;53(5):257–263.
8. Bashir MR, Bhatti L, Marin D, Nelson RC. Emerging applications for ferumoxytol as a contrast agent in MRI. J Magn Reson Imaging 2015;41(4):884–898.
9. Vasanawala SS, Nguyen KL, Hope MD, et al. Safety and technique of ferumoxytol administration for MRI. Magn Reson Med 2016;75(5):2107–2111.
10. Hope MD, Hope TA, Zhu C, et al. Vascular imaging with ferumoxytol as a contrast agent. AJR Am J Roentgenol 2015;205(3):W366–W373.
11. Hernando D, Kramer JH, Reeder SB. Multipeak fat-corrected complex R2* relaxometry: theory, optimization, and clinical validation. Magn Reson Med 2013;70(5):1319–1331.
12. Yu H, Shimakawa A, McKenzie CA, Brodsky E, Brittain JH, Reeder SB. Multiecho water-fat separation and simultaneous R2* estimation with multifrequency fat spectrum modeling. Magn Reson Med 2008;60(5):1122–1134.
13. Turkbey B, Agarwal HK, Shih J, et al. A Phase I Dosing Study of Ferumoxytol for MR Lymphography at 3 T in Patients With Prostate Cancer. AJR Am J Roentgenol 2015;205(1):64–69.
14. European Medicines Agency. Withdrawal assessment report for Sinerem. 2008. http://www.ema.europa.eu/docs/en_GB/document_library/Application_withdrawal_assessment_report/2010/01/WC500067463.pdf. Accessed January 15, 2019.
15. Storey P, Arbini AA. Bone marrow uptake of ferumoxytol: a preliminary study in healthy human subjects. J Magn Reson Imaging 2014;39(6):1401–1410.
16. Muehe AM, Feng D, von Eyben R, et al. Safety report of ferumoxytol for magnetic resonance imaging in children and young adults. Invest Radiol 2016;51(4):221–227.
17. Bashir MR, Mody R, Neville A, et al. Retrospective assessment of the utility of an iron-based agent for contrast-enhanced magnetic resonance venography in patients with endstage renal diseases. J Magn Reson Imaging 2014;40(1):113–118.
18. Schiller B, Bhat P, Sharma A. Safety and effectiveness of ferumoxytol in hemodialysis patients at 3 dialysis chains in the United States over a 12-month period. Clin Ther 2014;36(1):70–83.
19. Hetzel D, Strauss W, Bernard K, Li Z, Urboniene A, Allen LF. A Phase III, randomized, open-label trial of ferumoxytol compared with iron sucrose for the treatment of iron deficiency anemia in patients with a history of unsatisfactory oral iron therapy. Am J Hematol 2014;89(6):646–650.
20. Vadhan-Raj S, Strauss W, Ford D, et al. Efficacy and safety of IV ferumoxytol for adults with iron deficiency anemia previously unresponsive to or unable to tolerate oral iron. Am J Hematol 2014;89(1):7–12.
21. Macdougall IC, Strauss WE, McLaughlin J, Li Z, Dellanna F, Hertel J. A randomized comparison of ferumoxytol and iron sucrose for treating iron deficiency anemia in patients with CKD. Clin J Am Soc Nephrol 2014;9(4):705–712.
22. Auerbach M, Strauss W, Auerbach S, Rineer S, Bahrain H. Safety and efficacy of total dose infusion of 1,020 mg of ferumoxytol administered over 15 min. Am J Hematol 2013;88(11):944–947.